https://doi.org/10.5194/bg-2020-42
Preprint. Discussion started: 6 March 2020

Biogeosciences Discussions

Seasonal cycling of zinc and cobalt in the Southeast Atlantic along the GEOTRACES GA10 section.

Neil J. Wyatt[1], Angela Milne[2], Eric P. Achterberg[3], Thomas J. Browning[3], Heather A. Bouman[4], E. Malcolm S. Woodward[5], Maeve C. Lohan[1].

[1]Ocean and Earth Science, National Oceanography Centre, University of Southampton, Southampton, United Kingdom.

[2]School of Geography, Earth and Environmental Sciences, University of Plymouth, Plymouth, United Kingdom.

[3]Marine Biogeochemistry Division, GEOMAR Helmholtz Centre for Ocean Research, Kiel, Germany.

[4]Department of Earth Sciences, University of Oxford, Oxford, United Kingdom.

[5]Plymouth Marine Laboratory, Plymouth, United Kingdom.

Correspondence to: N. J. Wyatt (n.j.wyatt@soton.ac.uk)

Abstract

We report the distributions of dissolved zinc (dZn) and cobalt (dCo) in sub-tropical and sub-Antarctic waters of the Southeast Atlantic Ocean during austral spring 2010 and summer 2011/12. A strong seasonal signal was observed in sub-tropical surface waters with early spring mixed-layer dZn and dCo concentrations of 3.16 ± 1.35 nM and 39 ± 9 pM, respectively, compared with summer values depleted well below these levels by biological activity. The elevated spring mixed-layer dZn concentrations resulted from an apparent offshore transport of elevated dZn at depths between 20 – 50 m, derived from lithogenic inputs from the Agulhas

https://doi.org/10.5194/bg-2020-42
Preprint. Discussion started: 6 March 2020

Bank. In contrast, open-ocean sub-Antarctic surface waters displayed largely consistent inter-seasonal mixed-layer dZn and dCo concentrations of 0.11 ± 0.08 nM and 11 ± 5 pM, respectively. The vertical distributions of dZn and dCo in the upper water column were similar to that of phosphate (PO_4^{3-}), with positive linear relationships during each of the seasons and across dynamic biogeochemical regimes, suggesting surface biological drawdown and shallow remineralisation of these metals in this region largely influences their distribution. The ecological stoichiometries for dZn and dCo, calculated from the linear regression with PO_4^{3-}, suggest a greater overall use of dZn relative to dCo in the upper water column of the Southeast Atlantic with an inter-seasonal Zn:Co ratio ranging between 9 and 29. Sub-tropical surface water Zn:Co ratios were found to decrease between spring and summer indicating a preferential removal of dZn relative to dCo between seasons. In this paper we investigate how the seasonal influences of external input and phytoplankton succession may relate to the distribution of dZn and dCo, and variation in Zn:Co ecological stoichiometry, across two distinct ecological regimes in the Southeast Atlantic.

1. Introduction

The trace metal micronutrients zinc (Zn) and cobalt (Co) play an important role in the productivity of the oceans as key requirements in marine phytoplankton metabolism (Morel, 2008; Twining and Baines, 2013). Zinc is required for the acquisition of inorganic carbon and organic phosphorus via the carbonic anhydrase and alkaline phosphatase metalloenzymes, respectively (Morel et al., 1994; Shaked et al., 2006; Cox and Saito, 2013). The requirement for Co stems from its obligation in the biosynthesis of vitamin B_{12} (Raux et al., 2000; Rodionov et al., 2003) and, like Zn, its potential roles as a metal cofactor in carbonic anhydrase and alkaline phosphatase (Morel et al., 1994; Jakuba et al., 2008; Saito et al., 2017). Significantly, both dissolved Zn (dZn) and Co (dCo) are often scarce in surface seawater with mean

https://doi.org/10.5194/bg-2020-42
Preprint. Discussion started: 6 March 2020

concentrations that are often similar to, or relatively depleted, compared with typical biological requirements of phytoplankton (Moore et al., 2013; Moore, 2016). Hence, dZn and dCo availability have the potential to regulate phytoplankton metabolism and growth rates in some ocean regions (Sunda and Huntsman, 1992; Saito et al., 2002; Franck et al., 2003; Shaked et al., 2006; Bertrand et al., 2007; Jakuba et al., 2012; Mahaffey et al., 2014; Chappell et al., 2016; Browning et al., 2017).

The role for Zn and Co in carbonic anhydrase establishes an interaction between their ocean cycles, whereby biochemical substitutions between the enzyme-bound metals enables a stoichiometric plasticity in their cellular requirements that can negate the effect of limited availability. For example, a number of eukaryotic algae can substitute Zn for Co, as well as cadmium (Cd), in carbonic anhydrase when seawater dZn concentrations are low (Price and Morel, 1990; Sunda and Huntsman, 1995; Lane and Morel, 2000; Xu et al., 2007; Saito and Goepfert, 2008). In contrast, the prokaryotic picocyanobacteria *Synechococcus* and *Prochlorococcus* appear to have a near-absolute Co requirement (Sunda and Huntsman, 1995; Saito et al., 2002; Hawco and Saito, 2018). The availability and stoichiometry of dZn and dCo may therefore also exert a key control on phytoplankton community structure in some ocean regions (Leblanc et al., 2005; Saito et al., 2010; Chappell et al., 2016).

The Sub-Tropical Front (STF) of the Southeast Atlantic represents the convergence of warm, predominately macronutrient-limited Sub-Tropical Surface Water (STSW) and cold, iron-limited but macronutrient enriched Sub-Antarctic Surface Water (SASW), creating one of the most dynamic nutrient regimes in the oceans (Ito et al., 2005; Browning et al., 2014; Moore, 2016). Here, the relative supply and availability of macronutrients and iron (Fe) exert an important control in maintaining the elevated phytoplankton stock and productivity that is typical of this frontal region, particularly during austral spring and summer (Moore and Abbott, 2000; Ito et al., 2005; Browning et al., 2014). Dissolved Zn is also depleted in SASW that flows

https://doi.org/10.5194/bg-2020-42
Preprint. Discussion started: 6 March 2020

northwards to converge with STSW at the STF (Wyatt et al., 2014). However, the potential role for Zn in the mediation of phytoplankton distribution and community structure in this region is currently unclear.

Using data from two UK-GEOTRACES cruises (transect GA10) this study examines the seasonal availability and ecological stoichiometry of dZn and dCo, by analysis of their relationships with phosphate, in upper ocean waters of the Southeast Atlantic. These data, together with measurements of phytoplankton pigment biomass and community structure, offer an improved knowledge of the seasonal influences of external input and phytoplankton succession on the distribution and cycling of Zn and Co in these dynamic waters.

2. Methods

2.1. Sampling methods

Seawater samples were collected during two UK-GEOTRACES cruises in the South Atlantic Ocean (GA10, Fig. 1). The first cruise (D357) took place during austral spring 2010 (18th October to 22nd November 2010), sampling the Southeast Atlantic on-board the *RSS Discovery*. During D357, two transects were completed between Cape Town and the zero meridian that represent early austral spring (D357-1) and late austral spring (D357-2), respectively. The second cruise (JC068) took place during austral summer 2011/2012 (24th December 2011 to 27th January 2012), along the same transect of the first cruise and continuing along 40ºS between Cape Town and Montevideo, Uruguay, on-board the *RSS James Cook*. For JC068, we present here only the repeat transect data between Cape Town and 13°W that represents the Southeast Atlantic aspect of this transect.

All sampling bottles were cleaned according to the procedures detailed in the GEOTRACES sample handling protocols (Cutter et al., 2010). Seawater and particulate samples below 15 m depth were collected using a titanium-frame CTD with 24 trace metal clean 10 L Teflon-coated

https://doi.org/10.5194/bg-2020-42
Preprint. Discussion started: 6 March 2020

OTE (Ocean Test Equipment) Niskin bottles deployed on a plasma rope. Sub-samples for dissolved trace metal analysis were filtered through 0.8/0.2 µm cartridge filters (AcroPak™ 500, Pall) into 125 mL low density polyethylene bottles inside a class 1000 clean air container. Each sub-sample was acidified to pH 1.7 (0.024 M) by addition of 12 M hydrochloric acid (HCl, UpA, Romil) under a class 100 laminar flow hood. Vertical sampling for dissolved trace metals was augmented by surface samples collected at each station using a towed 'fish' positioned at approximately 3-5 m depth. Fish samples were filtered in-line and acidified as described for samples collected from the titanium sampling system. Particulate samples were collected onto acid clean 25 mm, 0.45 µm, polyethersulfone membrane disc filters (Supor®, Pall) and stored frozen (-20ºC) until shore-based analysis.

2.2. Trace metal analysis

Dissolved Co was determined in the ISO accredited clean room facility (ISO 9001) at the University of Plymouth (UK) using flow injection with chemiluminescence detection, modified from the method of Cannizzaro et al. (1999) as described by Shelley et al. (2010). Briefly, dCo was determined in UV-irradiated samples using the reaction between pyrogallol (1,2,3-trihydrobenzene) and hydrogen peroxide formed in the presence of Co. Standards (20 – 120 pM Co) were prepared in 0.2 µm filtered low-dCo seawater (16.5 ± 5.2 pM, n = 15) by serial dilution of a 1000 ppm Co ICP-MS standard (Romil, UK). The accuracy of the analytical method was validated by quantification of dCo in SAFe (S and D2) and GEOTRACES (GD) reference seawater (Table 1). The precision for triplicate analysis of each sample was between 1 and 5 %. There was no detectable analytical dCo blank and the limit of detection (3σ of the lowest standard addition) was 1.98 ± 0.87 pM.

Dissolved Zn was determined using flow injection coupled with fluorescence detection, modified from the method of Nowicki et al. (1994) and described previously for this

https://doi.org/10.5194/bg-2020-42
Preprint. Discussion started: 6 March 2020

GEOTRACES section by Wyatt et al. (2014). The accuracy of the analytical method was validated by quantification of dZn in SAFe (S and D2) reference seawater (Table 1). The precision for triplicate analysis of each sample was between 1 and 5 %. The blank for dZn FIA was 0.14 ± 0.13 nM and the limit of detection (3σ of the lowest standard addition) was 0.01 ± 0.01 nM.

Total particulate trace metals (i.e. pZn, pCo, pTi) were determined using inductively coupled plasma-mass spectrometry (Thermo Fisher XSeries-2) following a sequential acid digestion modified from Ohnemus et al. (2014). Potential interferences (e.g. $_{40}Ar_{16}O$ on $_{56}Fe$) were minimized through the use of a collision/reaction cell utilizing 7% H in He and evaluation of efficiency and accuracy assessed using Certified Reference Material (CRM). Full details of the method and CRM results can be found in Milne et al. (2017).

2.3. Nutrients, phytoplankton, temperature and salinity

The dissolved macronutrients phosphate (PO_4^{3-}), silicic acid ($Si(OH)_4$ but referred to as Si hereafter) and nitrate (determined as nitrate + nitrite, NO_3^-) were determined in all samples for which trace metals were determined, in addition to samples collected from a stainless steel rosette. Macronutrients were determined using an AA III segmented-flow AutoAnalyzer (Bran & Luebbe) following colorimetric procedures (Woodward and Rees, 2001). Salinity, temperature and depth were measured using a CTD system (Seabird 911+) whilst dissolved O_2 was determined using a Seabird SBE 43 O_2 sensor. Salinity was calibrated on-board using discrete samples taken from the OTE bottles and an Autosal 8400B salinometer (Guildline) whilst dissolved O_2 was calibrated using a photometric automated Winkler titration system (Carritt and Carpenter, 1966). Mixed-layer depths (MLD) were calculated using the threshold method of de Boyer Montégut et al. (2014), where MLD is identified from a linear interpolation

https://doi.org/10.5194/bg-2020-42
Preprint. Discussion started: 6 March 2020

between near-surface density and the depth at which density changes by a threshold value (0.125 kg m^{-3}).

Measurements of phytoplankton pigment biomass and community structure were made on discrete samples collected using a 24 position stainless-steel CTD rosette equipped with 20 L OTE Niskin bottles. For chlorophyll-*a* analysis, samples were filtered (0.7 µm Whatman GF/F) and then the filters extracted overnight in 90 % acetone (Holm-Hansen et al., 1965). The chlorophyll-*a* extract was measured on a pre-calibrated (spinach chlorophyll-*a* standard, Sigma) Turner Designs Trilogy fluorometer. High performance liquid chromatography (HPLC) samples (0.5 – 2 L) for accessory pigment analyses were filtered (0.7 µm Whatman GF/F), flash frozen in liquid nitrogen and stored at -80 °C prior to analysis using a Thermo HPLC system. The matrix factorization program CHEMTAX was used to estimate the contribution of taxonomic groups to total chlorophyll-*a* (Mackey et al., 1996). Concentrations of nanophytoplankton, *Synechococcus*, *Prochlorococcus* and photosynthetic picoeukaryotes were analysed by analytical flow cytometry (AFC) using a FACSort flow cytometer (Becton Dickenson, Oxford, UK) according to the methods described in Davey et al. (2008) and Zubkov et al. (2003).

3. Results and Discussion

3.1. Hydrographic setting and macronutrient distributions

The prominent waters masses along the D357 and JC068 transects (Fig. 2) were identified by their characteristic thermohaline and macronutrient properties (Sarmiento et al., 2004; Ansorge et al., 2005; Browning et al., 2014). Wyatt et al. (2014) provide a more detailed description of the JC068 hydrography along the entire GA10 section. Whilst we aim to compare the nearshore versus offshore distributions of micro- and macronutrients, note that Sub-Antarctic Mode

https://doi.org/10.5194/bg-2020-42
Preprint. Discussion started: 6 March 2020

174 Water was not largely sampled during the D357-2 late spring transect, and therefore only the
175 early spring and summer values are discussed for SASW hereafter.
176
177 ***Surface mixed-layer***
178 During all three transects the STF was identified by a sharp potential temperature (θ) gradient
179 in the upper 200 m with the θ 15°C isotherm corresponding well to changes in macronutrient
180 concentrations between STSW and SASW. North of the STF, mixed-layer macronutrient
181 concentrations (Table 2) decreased in STSW between the three transects. The largest depletion
182 observed was for NO_3^- with a 40-fold reduction in mean concentrations between early spring
183 and summer, whilst PO_4^{3-} and Si concentrations were reduced 1.7 and 2.1 fold, respectively.
184 Similarly, summer SASW mixed-layer mean concentrations of NO_3^-, PO_4^{3-} and Si were 1.8,
185 1.3 and 2.4 fold lower than early spring, respectively. The SASW mixed-layer concentrations
186 of NO_3^- and PO_4^{3-} were at least 2.5-fold higher than for STSW during the study, whilst the Si
187 concentration was at least 1.5-fold lower, highlighting the relative deficiencies in major
188 nutrients between high and low latitude derived surface waters (Sarmiento et al., 2004; Moore,
189 2016).
190
191 ***Sub-surface waters***
192 The Southern Ocean derived Sub-Antarctic Mode Water (SAMW) and underlying Antarctic
193 Intermediate Water (AAIW) were identified using their characteristic core potential density
194 (σθ 26.8 kg m^{-3}) (Sarmiento et al., 2004; Palter et al., 2010) and thermohaline (S <34.4, θ
195 >2.8ºC) properties (Fig. 2). Wyatt et al. (2014) have identified these water masses along this
196 section between 200 and 500 m. During all three transects, low sub-surface (50 – 500 m)
197 macronutrient concentrations were observed between 13 and 16°E, associated with a salinity
198 maxima. The feature conforms to the mean locality and depth range of Agulhas water

https://doi.org/10.5194/bg-2020-42
Preprint. Discussion started: 6 March 2020

(Duncombe Rae, 1991), clearly highlighting the penetration of Indian Ocean water into northward flowing SAMW.

3.2. Zn and Co distributions of the Southeast Atlantic Ocean

Surface mixed-layer

Figure 3 shows the dZn and dCo distributions for the upper 500 m of the Southeast Atlantic for the D357 and JCO68 transects. Here, surface mixed-layer dZn and dCo concentrations ranged from 0.01 – 4.57 nM and 1 – 50 pM, respectively. The large range in dZn concentrations resulted from an apparent offshore transport of elevated dZn within STSW between 20 – 50 m during early spring (1.48 – 4.57 nM; Stns. 1 – 2) that was reduced by late spring (0.48 – 1.76 nM; Stns. 0.5 – 1.5) and was absent during summer (0.01 – 0.13 nM; Stns. 1 – 2). Similarly, but to a lesser extent, elevated dCo concentrations were observed in STSW between 10 and 50 m during early and late spring (15 – 50 pM), compared with summer (18 – 33 pM). Our findings are consistent with previous observations of elevated dissolved and particulate trace metals over the same depth range in waters close to South Africa, including Co, Fe, Mn, and Pb (Chever et al., 2010; Bown et al., 2011; Boye et al., 2012; Paul et al., 2015). We postulate that these trace metal enrichments can arise from either atmospheric inputs, and/or from the lateral advection of metal-enriched waters from the Agulhas Current (AC) and/or South African continental shelf. Chance et al. (2015) identified the air masses for D357 and JC068 as 'remote South Atlantic air' with metal loadings comparable with this air class. With only brief, light rain encountered during the transects, thus minimal wet deposition of atmospheric aerosol, Chance et al. (2015) provide modest dry deposition flux estimates of 0.6 – 6.0 and 0.02 – 0.05 nmol m^{-2} d^{-1} for soluble Zn and Co respectively. Thus, we propose that the offshore advection of water masses enriched in trace metals can form a source to the surface waters of the Southeast Atlantic and discuss this further in Sect. 3.2.1. In SASW, mixed-layer dZn and dCo

https://doi.org/10.5194/bg-2020-42
Preprint. Discussion started: 6 March 2020

concentrations ranged from 0.01 to 0.25 nM and 3 to 18 pM, respectively, during the study, significantly lower than STSW values, with the lowest concentrations observed during the summer transect (Table 2).

Sub-surface waters

During the early spring D357-1 transect, elevated dZn and dCo concentrations were observed between the surface mixed-layer and 500 m (1.48–3.85 nM and 39–62 pM, respectively) at the station closest the South African continent (Stn. 1). Here, the highest dZn concentrations were associated with the dZn-enriched waters (20–50 m) described above for the surface mixed-layer. During the late spring D357-2 transect, the near-shore (Stns. 0.5–1) dZn concentrations were lower (0.31–1.76 nM) whilst dCo remained similar to early spring values (27–57 pM). During summer, near-shore (Stn. 1) sub-surface dZn concentrations were markedly lower (0.03–0.50 nM) than spring values whilst dCo concentrations (17–52 pM) were only marginally lower. In offshore waters, sub-surface dZn concentrations ranged 0.01–1.01 nM across all three transects with extremely low values in the upper 400 m (0.22 ± 0.21 nM) and the highest values between 400 and 500 m. The absence of a significant return path for dZn with SAMW to waters above 400 m at this latitude (Wyatt et al., 2014; Vance et al., 2017) is likely an important control on dZn distributions across all three transects. In contrast, dCo concentrations were depleted in the upper 200 m (1–35 pM) and elevated in SAMW (23–56 pM) suggesting that these Southern Ocean derived waters also play an important role in upper water column dCo distributions of the South Atlantic.

3.3. Shelf derived sources of Zn and Co

Potential sources of trace metals to surface waters of the Southeast Atlantic include atmospheric inputs from South Africa and Patagonia (Chance et al., 2015; Menzel Barraqueta

https://doi.org/10.5194/bg-2020-42
Preprint. Discussion started: 6 March 2020

et al., 2019) as well as interactions with shelf and slope waters of the Agulhas Bank (Bown et al., 2011; Boye et al., 2012; Paul et al., 2015). During the D357 spring transects, elevated mixed-layer dZn and dCo concentrations (up to 4.57 nM and 50 pM, respectively; Sect. 3.2) were observed at stations closest the Agulhas Bank shelf and slope (Stns. 0.5, 1, 1.5 and 2). Here, we compare these metal elevations with respect to the aforementioned sources. Firstly, we encountered only brief, light rain during the study, thus minimal wet deposition of atmospheric aerosol. By combining the median atmospheric dry deposition flux for soluble Zn and Co for the Southeast Atlantic (Zn 6.0 and Co 0.05 nmol m^{-2} d^{-1}; Chance et al., 2015) with the mean mixed-layer depth (34 m) for STSW during D357, dust dissolution is estimated to add up to 5.5 pM dZn and 0.05 pM dCo over a one month period. These inputs are low compared with the mixed-layer metal inventories, representing <1 % of dZn and dCo in STSW during the D357 transects (Table 2), and would not be sufficient to generate distinct mixed-layer maxima. It is likely, therefore, that the dZn and dCo elevations originated from the advection of metal-enriched waters from the western Agulhas Bank, a region identified as a distinct source of both dissolved and particulate trace metals to the Southeast Atlantic (Chever et al., 2010; Bown et al., 2011; Boye et al., 2012; Paul et al., 2015), and/or from the leakage of Indian Ocean water into the Southeast Atlantic via the AC.

The detachment of Agulhas rings and filaments from the AC during its retroflection back towards the Indian Ocean constitutes a source of Pb to the surface Southeast Atlantic along the D357 transects (Paul et al., 2015). Whilst we observed elevated mixed-layer dZn and dCo at ~15ºE during both D357 transects, the absence of metal enrichment across the depth of the AC salinity maxima (Figs. 2 and 3) suggests that the signal must be entrained from elsewhere. Furthermore, dZn concentrations from the AC along the east coast of South Africa do not exceed 0.5 nM in the upper 200 m (Gosnell et al., 2012). It is therefore likely that the dZn and dCo enrichment was derived from the Agulhas Bank. The AC has been shown to meander over,

https://doi.org/10.5194/bg-2020-42
Preprint. Discussion started: 6 March 2020

and interact with, the Agulhas Bank, forming eddies and filaments on the shoreward edge of the AC proper, that tend to move northwards along the western shelf edge and into the Southeast Atlantic (Lutjeharms and Cooper, 1996; Lutjeharms, 2007), potentially delivering shelf-derived lithogenic material. We found no evidence of a fluvial signature in our data, and no significant fluvial source for trace elements to our study region has been reported in the literature. Whilst we cannot exclude an uncharacterized fluvial input, we focus here on the more likely scenario of sedimentary, lithogenic inputs as the driver of mixed-layer dZn and dCo elevations at the shelf and slope stations during D357. Despite no available particulate trace metal data for the D357-1 early spring transect for direct comparison with the highest dZn and dCo elevations, we observed elevated mixed-layer particulate Zn (pZn; 0.08–1.4 nM) and Co (pCo; 8–42 pM) at stations 0.5, 1 and 1.5 during the D357-2 late spring transect (Fig. S1), coincident with elevated dZn (0.05–1.82 nM) and dCo (1–43 pM). In addition, we found a strong positive correlation between particulate aluminium (pAl) and titanium (pTi) (pAl/pTi; slope 41.7 M:M; Pearson's *r* 0.99, n = 15) as well as particulate Fe (pFe/pTi; slope 10.2 M:M; Pearson's *r* 0.99, n = 15) for the upper 500 m at stations closest South Africa (Stns. 0.5 and 1) during D357-2, indicative of a strong lithogenic source. The slopes of these relationships are in excess of the upper crustal mole ratios of 34.1 and 7.3 for Al/Ti and Fe/Ti, respectively (McLennan, 2001). Given the refractory nature of lithogenic pTi across diverse oceanic environments (Ohnemus and Lam, 2015), this may suggest an additional supply of Al and Fe via resuspension of Agulhas Bank sediments followed by westward offshore transport, a common feature of the Bank's physical circulation during spring and summer (Largier et al., 1992). Such processes may in turn provide an additional source of Zn and Co to STSW of the Southeast Atlantic. Indeed, Little et al. (2016) proposed that oxygen-deficient, organic-rich, continental margin sediments may constitute a significant global sink for Zn. In turn, this could provide a local source following resuspension. Furthermore, recent model outputs have

https://doi.org/10.5194/bg-2020-42
Preprint. Discussion started: 6 March 2020

299 highlighted low oxygen, boundary sediments as a dominant external source of Co to the oceans
300 (Tagliabue et al., 2018). Given that oxygen depleted (<1 ml/L) bottom waters are prevalent
301 across the western Agulhas Bank (Chapman and Shannon, 1987; Chapman, 1988), considered
302 to arise from high organic matter input to sediments and its bacterial decomposition, a
303 sedimentary lithogenic source of Zn and Co appears likely.
304

305 **3.4. Trace metal ecological stoichiometry of the upper Southeast Atlantic**

306 In addition to seasonal variations in the lateral advection of continentally derived trace metals,
307 the lower dZn and dCo concentrations in STSW during summer, compared with spring, likely
308 reflect differences in biological utilisation. Linear correlations between soluble reactive
309 phosphate (PO_4^{3-}) and dissolved Zn and Co have been reported as evidence for biological
310 uptake and remineralisation (Wyatt et al., 2014; Saito et al., 2017), with the aggregate slope of
311 these relationships representative of the two processes on metal biogeochemistry. Here, we
312 examine the slopes of metal/PO_4^{3-} from simple linear regression to assess the 'ecological
313 stoichiometry' of the Southeast Atlantic over seasonal timescales. The data were grouped into
314 STSW and SASW regimes, separated by the STF, and regression analysis performed between
315 the surface ocean and the depth that metal/PO_4^{3-} remained linear (Table 2). The continentally
316 derived excess dZn and dCo observed in STSW during early and late spring were removed
317 from the regression analysis in order to compare ecological stoichiometry with respect to
318 biological processes. For SASW, micronutrient sampling did not occur during late spring and
319 therefore only early spring and summer values are compared.
320 Distinct temporal trends in the stoichiometric relationship with PO_4^{3-} were evident for both dZn
321 and dCo (Fig. 4). Strong, positive metal/PO_4^{3-} correlations were observed for the upper water
322 column (Table 2), highlighting the importance of micronutrient processes with respect to the
323 organization of dZn and dCo. Within STSW, dZn/PO_4^{3-} ranged from 274 to 1150 µM:M (r

https://doi.org/10.5194/bg-2020-42
Preprint. Discussion started: 6 March 2020

0.56–0.69), with the steepest slope observed during early spring and the shallowest slope during summer. Combined with the low summer dZn concentration for STSW, this suggests strong biological uptake of dZn between seasons. In contrast, consistently shallow dZn/PO_4^{3-} slopes of 276 and 302 µM:M (r 0.59–0.76) were observed in SASW during early spring and summer, respectively.

A similar spatiotemporal variation was observed for dCo/PO_4^{3-} with slopes ranging from 24 to 39 µM:M (*r* 0.62–0.83). These values are broadly similar to the range of dCo/PO_4^{3-} stoichiometries reported over similar depths across the equatorial and South Atlantic (27–53 µM:M; Saito et al. 2017, and references therein). Steeper slopes have been reported across the North Atlantic (~41–560 µM:M; Saito and Moffett, 2002; Dulaquais et al., 2014; Noble et al., 2017; Saito et al., 2017), likely reflecting an elevated atmospheric Co input and/or an extremely low surface PO_4^{3-} inventory (Wu et al., 2000; Martiny et al., 2019). Like dZn, the steepest dCo/PO_4^{3-} slope of 39 µM:M was observed in STSW during early spring with slopes of 28 and 24 µM:M observed during late spring and summer, respectively, reflecting preferential trace metal removal relative to PO_4^{3-} between the seasons. In contrast to STSW, it would appear that PO_4^{3-} is preferentially removed over dZn and dCo in SASW between early spring and summer, potentially reflecting the greater availability of PO_4^{3-} in these Southern Ocean derived waters (Table 2) and an open-ocean phytoplankton community that have lower trace metal requirements than their counterparts north of the STF.

Our results provide evidence for the preferential removal and greater overall use of dZn relative to dCo in STSW of the Southeast Atlantic, based on Zn:Co stoichiometries (dZn/PO_4^{3-}:dCo/PO_4^{3-}) of 29, 23 and 11 for the three transects (Table 2). In contrast, the stoichiometry of SASW was remarkably consistent between transects with a Zn:Co ratio of 9 for both early spring and summer, indicating a more balanced ecophysiological regime with regard to dZn and dCo organisation. We postulate that the inter-seasonal variations in dZn and dCo

https://doi.org/10.5194/bg-2020-42
Preprint. Discussion started: 6 March 2020

availability and stoichiometry of the Southeast Atlantic reflect changes in the relative nutritional requirement of resident phytoplankton and/or biochemical substitution of Co and Zn to meet nutritional demand.

3.5. Phytoplankton controls on trace metal ecological stoichiometry

Here we discuss the principle, inter-linked phenomena that together likely explain our observations of seasonally decreasing Zn:Co stoichiometries in STSW of the Southeast Atlantic: i.e. the preferential removal of dZn, relative to dCo, leading to low dZn availability, and differences in phytoplankton assemblages with different cellular metal requirements.

First, the depletion of dZn by phytoplankton (the summer STSW mixed-layer dZn inventory was 11.5 % that of early spring, Table 2) could result in a lower Zn demand, relative to Co, and thus induce the negative trajectory of Zn:Co through microbial loop remineralisation. This postulation is supported by field and laboratory evidence that Zn:Co, as well as Zn:Cd, uptake rates in certain species of eukaryotic phytoplankton are positively correlated with Zn availability (Sunda and Huntsman, 1995, 1998, 2000; Cullen and Sherrell, 2005; Xu et al., 2007). Second, and largely connected to carbonic anhydrase, several species of eukaryotic phytoplankton have a Zn requirement that can be partially replaced by Co or Cd to maintain optimal growth rates (Price and Morel, 1990; Sunda and Huntsman, 1995; Lee and Morel, 1995; Lane and Morel, 2000; Xu et al., 2007; Saito and Goepfert, 2008). For example, species of the widespread haptophyte genus *Phaeocystis* appear to have a preferential Zn requirement and the capability to metabolically substitute Zn for Co (Saito and Goepfert, 2008), as do certain coastal and oceanic diatoms (Price and Morel, 1990; Sunda and Huntsman, 1995; Lane and Morel, 2000). Conversely, the ubiquitous haptophyte *Emiliania huxleyi* has a preferential Co requirement that can be partly met by Zn (Sunda and Huntsman, 1995; Xu et al., 2007), whilst in stark contrast, the picocyanobacteria *Prochlorococcus* and *Synechococcus* have near-

https://doi.org/10.5194/bg-2020-42
Preprint. Discussion started: 6 March 2020

absolute Co requirements (Sunda and Huntsman, 1995; Saito et al., 2002). Thus, inter-seasonal changes in phytoplankton biomass and composition, inherently related to metal availability, have the potential to alter the dissolved phase stoichiometry through uptake and remineralisation.

Satellite images show elevated surface chlorophyll concentrations across the Southeast Atlantic STF, compared with waters further north and south, with peak concentrations observed during summer in January 2012 (Fig. 1). Profiles of total chlorophyll-*a* concentration (Fig. S2) also show maximum summer values in the upper water column of STSW (1.02 mg m^{-3}) and SASW (0.49 mg m^{-3}) compared with spring values (<0.61 and <0.36 mg m^{-3}, respectively). This is consistent with the hypothesis that increasing irradiance, coupled with shallower mixed-layer depths (de Boyer Montégut et al., 2004), results in enhanced growth conditions leading to an increase in chlorophyll-*a* concentrations across the STF between September and February (Browning et al., 2014). Diagnostic pigment analyses (Fig. 5a) indicated that *Phaeocystis*-type haptophytes dominated the early spring STSW chlorophyll-*a* content (73 %) but with a reduced contribution during summer (20 %). Maximum growth rates for cultured *Phaeocystis antarctica* have been achieved under elevated Zn concentrations (Saito and Goepfert, 2008), and thus, the dominance of this haptophyte would likely contribute to the preferential removal of dZn between spring and summer. Furthermore, an increased summer diatom contribution (13 % chlorophyll-*a* compared with near zero during spring transects) would further reduce the dZn inventory, with diatoms having at least four-fold higher cellular Zn:P ratios than co-occurring cell types (Twining and Baines, 2013). The fact that both *Phaeocystis* and diatoms maintain a contribution to the summer STSW chlorophyll-*a* complement, when dZn availability is low, is intriguing. Both *Phaeocystis antarctica* and the larger, coastal diatoms *Thalassiosira pseudonana* and *Thalassiosira weissflogii* have been shown to be growth limited in culture by free Zn^{2+} concentrations ≤10 pM in the absence of Co (Sunda and Huntsman,

https://doi.org/10.5194/bg-2020-42
Preprint. Discussion started: 6 March 2020

1992; Saito and Goepfert, 2008). A simple estimate of summer STSW mixed-layer free Zn^{2+} availability, based on North Atlantic organic complexation data (>96 %; Ellwood and Van den Berg, 2000), indicates Zn^{2+} could have ranged between 3 and 11 pM, suggesting the potential for growth limitation of these phytoplankton. In addition, when comparing the Southeast Atlantic dZn stoichiometry with the cellular requirements of phytoplankton (Fig. 6) grown under growth rate limiting conditions (Sunda and Huntsman, 1995), analogous to the comparison by Saito et al. (2010) for the Ross Sea, we found summer STSW dZn/PO_4^{3-} to be in deficit of the requirements of the large diatom *T. pseudonana* but not those of the smaller diatom *T. oceanica*. The variation in cellular Zn:P between small and large phytoplankton is related to the higher surface-area-to-volume ratio of smaller cells, and the limitation of diffusive uptake rates at low Zn^{2+} concentrations (Sunda and Huntsman, 1995). This would suggest that the low dZn availability in summer STSW could influence phytoplankton species composition by selecting for smaller organisms with lower cellular Zn requirements. The comparison further implies that the presence of *Phaeocystis* and diatoms in summer STSW may be linked with their metabolic Zn-Co-Cd substitution capability, potentially allowing them to overcome some portion of their Zn deficiency. For example, Saito and Goepfert (2008) reported increased growth rates for *P. antarctica* grown at Zn^{2+} <1 pM following the addition of Co, whilst increased Co and/or Cd uptake has been observed by the diatoms *T. pseudonana* and *T. weissflogii* grown at Zn^{2+} <3 pM (Sunda and Huntsman, 1995, 1998, 2000). Thus, the lower Co/PO_4^{3-} of summer STSW, relative to spring, may be in part related to enhanced dCo uptake resulting from the need for biochemical substitution alongside the growth of phytoplankton with distinct Co requirements.

In contrast to *Phaeocystis*, *E. huxleyi*-type haptophytes were near-absent in spring STSW (<5 % chlorophyll-*a*; Fig. 5a) and increased in contribution during summer (18 %). *Emiliania huxleyi* appear to have a biochemical preference for Co over Zn (Xu et al., 2007), which could

https://doi.org/10.5194/bg-2020-42
Preprint. Discussion started: 6 March 2020

potentially be a contributing factor to the increased fraction of this haptophyte in summer STSW. Based on Co organic complexation data for Southeast Atlantic STSW (>99 %; Bown et al., 2012), however, even the maximum mixed-layer dCo concentration of 50 pM (estimated free Co^{2+} <0.5 pM) observed for this entire study would be sufficient to limit the growth of cultured *E. huxleyi* in the absence of Zn or Cd (Sunda and Huntsman, 1995; Xu et al., 2007). Despite this, Xu et al. (2007) showed that *E. huxleyi* can maintain significant growth at only 0.3 pM Co^{2+} in the presence of Zn, with the limitation by, and substitution of these metals reported to occur over a range of free ion concentrations (0.2–5 pM) that is relevant to summer conditions of the Southeast Atlantic. This assessment implies an additional need for Zn in phytoplankton nutrition due to low dCo availability throughout the Southeast Atlantic, which may further induce the negative trajectory of Zn:Co through microbial loop remineralisation.

In contrast to nanophytoplankton, the elevated summer STSW chlorophyll-*a* concentrations were accompanied by increased cell concentrations of *Synechococcus* and *Prochlorococcus* (>100 cells μL^{-1}) relative to spring abundance (Fig. 5a). This pattern suggests an inter-seasonal community shift towards smaller picocyanobacterial cells that is coincident with a decreased dZn stoichiometry. *Synechococcus* and *Prochlorococcus* are thought to have little or no Zn requirement and relatively low Co requirements (growth limited by ≤0.2 pM Co^{2+}; Sunda and Huntsman, 1995; Saito et al., 2002). This, alongside their small cell size, hence greater capacity for acquiring fixed nitrogen under conditions where this nutrient is strongly depleted, may allow these prokaryotes to flourish following depletion and export of Zn associated with *Phaeocystis* and diatom blooms. This supposition is supported by observations of a persistently high abundance of *Synechococcus* and *Prochlorococcus* (>1000 cells μL^{-1}) relative to eukaryotic nanophytoplankton in the higher nitrate but dZn depleted surface waters of the Costa Rica Dome (Saito et al., 2005; Ahlgren et al., 2014; Chappell et al., 2016), where surface dCo concentrations were maintained above that of surrounding waters by the biological production

https://doi.org/10.5194/bg-2020-42
Preprint. Discussion started: 6 March 2020

of Co-binding ligands (Saito et al., 2005). The increased abundance of these prokaryotic autotrophs in summer STSW of the Southeast Atlantic may have also contributed to the inter-seasonal negative trajectory of dCo/PO_4^{3-} slopes. In contrast to STSW, cells counts of eukaryotic phytoplankton and prokaryotic cyanobacteria in SASW varied little between spring and summer (Fig. 5b), consistent with a near-constant Zn:Co stoichiometry, and indicative of a more balanced ecophysiological regime. The fractional contribution of *Phaeocystis* (Fig. 5a), the dominant contributor to the SASW chlorophyll-*a* complement, was similar between transects at 54 and 44 %, respectively, whilst the contribution of *E. huxleyi* increased from 19 to 33 % between spring and summer, respectively. Whilst it is proposed that the low supply rate of Fe to these waters provides a dominant control on phytoplankton biomass and composition (Browning et al., 2014), low dZn and dCo availability may also be an important driver of such changes. Indeed, the SASW mixed-layer dZn and dCo concentrations (0.11 ± 0.08 nM and 11 ± 5 pM, respectively) during this study were similar to, or below, the requirements of *Phaeocystis* and *E. huxleyi* in the absence of cambialistic metabolism (Saito and Goepfert, 2008). The presence of these phytoplankton in summer SASW therefore provides evidence for Zn and Co, and potentially Cd, biochemical substitution in oceanic waters of the Southeast Atlantic. Conversely, the absence of a significant diatom contribution to summer SASW chlorophyll-*a* (Fig. 5a), relative to early spring, does not reflect the cellular Zn requirement of typical oceanic diatoms (Fig. 6), and may be instead related to low Fe availability and stress-induced Si exhaustion. In support of this, we calculate summer SASW mixed-layer Si concentrations (0.8 ± 0.4 μM) to be <50 % of early spring values (1.8 ± 0.2 μM) and a dissolved NO_3^-:Si stoichiometry of 3.8:1 close to the 4:1 shown to limit diatom growth in culture (Gilpin et al., 2004), and in contrast to the 0.4:1 calculated for early spring.

3.6. Conclusion

https://doi.org/10.5194/bg-2020-42
Preprint. Discussion started: 6 March 2020

We report the distributions of dZn and dCo in the upper water column of sub-tropical and sub-Antarctic waters of the Southeast Atlantic during austral spring and summer periods. We identify an apparent continental source of dZn and dCo to sub-tropical waters at depths between 20 – 50 m, derived from lithogenic inputs from the Agulhas Bank. In contrast, open-ocean sub-Antarctic surface waters displayed largely consistent inter-seasonal mixed-layer dZn and dCo concentrations indicating a more balanced ecophysiological regime with regard to their organisation. The vertical distributions of dZn and dCo in the upper water column were similar to that of PO_4^{3-} with positive metal/PO_4^{3-} slopes observed during each of the seasons and across dynamic biogeochemical regimes, indicating biological drawdown and shallow remineralisation of these metals in this region significantly influences their distribution.

Absolute trace metal concentrations alongside ecological stoichiometries, calculated from linear regression with PO_4^{3-}, suggest the preferential utilization of dZn, relative to dCo, in the Southeast Atlantic with Zn:Co ranging between 9 and 29 during the study. The inter-seasonal removal of dZn results in summer concentrations that are potentially growth limiting for certain phytoplankton species estimated to be present in these waters by diagnostic pigment analyses. We therefore suggest cambialistic metabolic substitution between Zn and Co, and potentially Cd, is an important factor regulating the growth, distribution and diversity of phytoplankton in the Southeast Atlantic.

Data availability. The trace metal and macronutrient data sets used for analyses in this study are available at https://www.bodc.ac.uk/geotraces/data/idp2017/ (GEOTRACES GA10) and phytoplankton data at https://www.bodc.ac.uk/.

Competing interests. The authors declare that they have no conflict of interest.

https://doi.org/10.5194/bg-2020-42
Preprint. Discussion started: 6 March 2020

Author contribution. MCL and EPA acquired the funding. NJW, MCL, AM, TJB, EMSW, and HAB collected samples at sea. NJW conducted the Zn and Co measurements, EMSW the macronutrient measurements and TJB the phytoplankton measurements. NJW prepared the manuscript with significant contributions from all co-authors.

Acknowledgments. We thank the officers, crew, technicians and scientists of the *RRS James Cook* for their help on the UK-GEOTRACES D357 and JC068 cruises. This work was funded by the UK-GEOTRACES National Environmental Research Council (NERC) Consortium Grant (NE/H006095/1 (MCL & HAB) & NE/H004475/1 (EPA)).

References

Ahlgren, N. A., Noble, A. E., Patton, A. P., Roache-Johnson, K., Jackson, L., Robinson, D., McKay, C., Moore, L. R., Saito, M. A., and Rocap, G.: The unique trace metal and mixed layer conditions of the Costa Rica upwelling dome support a distinct and dense community of Synechococcus, Limnol. Oceanogr., 59, 2166-2184, doi:10.4319/lo.2014.59.6.2166, 2014.

Ansorge, I. J., Speich, S., Lutjeharms, J. R. E., Goni, G. J., Rautenbach, C. J. D., Froneman, P. W., Rouault, M., and Garzoli, S.: Monitoring the oceanic flow between Africa and Antarctica: Report of the first Goodhope cruise, S. Afr. J. Sci., 101, 29-35, 2005.

Bertrand, E. M., Saito, M. A., Rose, J. M., Riesselman, C. R., Lohan, M. C., Noble, A. E., Lee, P. A., and DiTullio, G. R.: Vitamin b12 and iron colimitation of phytoplankton growth in the Ross Sea, Limnol. Oceanogr., 52, 1079-1093, doi:10.4319/lo.2007.52.3.1079, 2007.

Bown, J., Boye, M., Baker, A., Duvieilbourg, E., Lacan, F., Le Moigne, F., Planchon, F., Speich, S., and Nelson, D. M.: The biogeochemical cycle of dissolved cobalt in the Atlantic and the Southern Ocean south off the coast of South Africa, Mar. Chem., 126, 193-206, doi:10.1016/j.marchem.2011.03.008, 2011.

Bown, J., Boye, M., and Nelson, D. M.: New insights on the role of organic speciation in the biogeochemical cycle of dissolved cobalt in the southeastern Atlantic and the Southern Ocean, Biogeosciences, 9, 2719–2736, doi:10.5194/bg-9-2719-2012, 2012.

Boye, M., Wake, B. D., Garcia, P. L., Bown, J., Baker, A. R., and Achterberg, E. P.: Distributions of dissolved trace metals (Cd, Cu, Mn, Pb, Ag) in the southeastern Atlantic and the Southern Ocean, Biogeosciences, 9, 3231-3246, doi:10.5194/bg-9-3231-2012, 2012.

https://doi.org/10.5194/bg-2020-42
Preprint. Discussion started: 6 March 2020

530 Browning, T. J., Bouman, H. A., Moore, C. M., Schlosser, C., Tarran, G. A., Woodward, E.
531 M. S., and Henderson, G. M.: Nutrient regimes control phytoplankton ecophysiology in the
532 South Atlantic, Biogeosciences, 11, 463-479, doi:10.5194/bg-11-463-2014, 2014.

533 Browning, T. J., Achterberg, E. P., Rapp, I., Engel, A., Bertrand, E. M., Tagliabue, A., and
534 Moore, C. M.: Nutrient co-limitation at the boundary of an oceanic gyre, Nature, 551, 242-246,
535 doi:10.1038/nature24063, 2017.

536 Cannizzaro, V., Bowie, A.R., Sax, A., Achterberg, E. P., Worsfold, P. J.: Determination of
537 cobalt and iron in estuarine and coastal waters using flow injection with chemiluminescence
538 detection, Analyst, 125, 51-57, doi:10.1039/A907651d, 2000.

539 Carritt, D. E., and Carpenter, J. H.: Comparison and evaluation of currently employed
540 modifications of the Winkler method for determining dissolved oxygen in seawater; a nasco
541 report, J. Mar. Res., 24, 286 - 319, 1966.

542 Chance, R., Jickells, T. D., and Baker, A. R.: Atmospheric trace metal concentrations,
543 solubility and deposition fluxes in remote marine air over the south-east Atlantic, Mar. Chem.,
544 177, 45-56, doi:10.1016/j.marchem.2015.06.028, 2015.

545 Chapman, P.: On the occurrence of oxygen-depleted water south of Africa and its implications
546 for Agulhas-Atlantic mixing, S. Afr. J. Marine Sci., 7, 267-294,
547 doi:10.2989/025776188784379044, 1988.

548 Chapman, P., and Shannon, L. V.: Seasonality in the oxygen minimum layers at the extremities
549 of the Benguela system, S. Afr. J. Marine Sci., 5, 85-94, doi:10.2989/025776187784522162,
550 1987.

551 Chappell, P. D., Vedmati, J., Selph, K. E., Cyr, H. A., Jenkins, B. D., Landry, M. R., and
552 Moffett, J. W.: Preferential depletion of zinc within Costa Rica upwelling dome creates
553 conditions for zinc co-limitation of primary production, J. Plankton Res., 38, 244-255,
554 doi:10.1093/plankt/fbw018, 2016.

555 Chever, F., Bucciarelli, E., Sarthou, G., Speich, S., Arhan, M., Penven, P., and Tagliabue, A.:
556 Physical speciation of iron in the Atlantic sector of the Southern Ocean along a transect from
557 the subtropical domain to the Weddell Sea Gyre, J. Geophys. Res-Oceans, 115, C10059,
558 doi:10.1029/2009jc005880, 2010.

559 Cox, A., and Saito, M.: Proteomic responses of oceanic Synechococcus WH8102 to phosphate
560 and zinc scarcity and cadmium additions, Front Microbiol, 4, doi:10.3389/fmicb.2013.00387,
561 2013.

562 Cullen, J. T., and Sherrell, R. M.: Effects of dissolved carbon dioxide, zinc, and manganese on
563 the cadmium to phosphorus ratio in natural phytoplankton assemblages, Limnol. Oceanogr.,
564 50, 1193-1204, doi:10.4319/lo.2005.50.4.1193, 2005.

565 Davey, M., Tarran, G. A., Mills, M. M., Ridame, C., Geider, R. J., and LaRoche, J.: Nutrient
566 limitation of picophytoplankton photosynthesis and growth in the tropical North Atlantic,
567 Limnol. Oceanogr., 53, 1722–1733, doi:10.4319/lo.2008.53.5.1722, 2008

https://doi.org/10.5194/bg-2020-42
Preprint. Discussion started: 6 March 2020

568 de Boyer Montégut, C., Madec, G., Fischer, A. S., Lazar, A., and Iudicone, D.: Mixed layer
569 depth over the global ocean: An examination of profile data and a profile-based climatology,
570 J. Geophys. Res-Oceans, 109, C12003, doi:10.1029/2004jc002378, 2004.

571 Dulaquais, G., Boye, M., Middag, R., Owens, S., Puigcorbe, V., Buesseler, K., Masqué, P.,
572 Baar, H. J., and Carton, X.: Contrasting biogeochemical cycles of cobalt in the surface western
573 Atlantic Ocean, Global Biogeochem. Cy., 28, 1387–1412, doi:10.1002/2014GB004903, 2014.

574 Duncombe Rae, C. M.: Agulhas retroflection rings in the South Atlantic Ocean: An overview,
575 S. Afr. J. Marine Sci., 11, 327-344, doi:10.2989/025776191784287574, 1991.

576 Ellwood, M. J., and Van den Berg, C. M. G.: Zinc speciation in the Northeastern Atlantic
577 Ocean, Mar. Chem., 68, 295-306, doi:10.1016/S0304-4203(99)00085-7, 2000.

578 Franck, V. M., Bruland, K. W., Hutchins, D. A., and Brzezinski, M. A.: Iron and zinc effects
579 on silicic acid and nitrate uptake kinetics in three high-nutrient, low-chlorophyll (HNLC)
580 regions, Mar. Ecol. Prog. Ser., 252, 15-33, doi:10.3354/meps252015, 2003.

581 Gilpin, L. C., Davidson, K., and Roberts, E.: The influence of changes in nitrogen: silicon ratios
582 on diatom growth dynamics, J. Sea Res., 51, 21-35, doi:10.1016/j.seares.2003.05.005, 2004.

583 Gosnell, K. J., Landing, W. M., and Milne, A.: Fluorometric detection of total dissolved zinc
584 in the southern Indian Ocean, Mar. Chem., 132, 68-76, doi:10.1016/j.marchem.2012.01.004,
585 2012.

586 Hawco, N. J., and Saito, M. A.: Competitive inhibition of cobalt uptake by zinc and manganese
587 in a Pacific Prochlorococcus strain: Insights into metal homeostasis in a streamlined
588 oligotrophic cyanobacterium, Limnol. Oceanogr., 63, 2229-2249, doi:10.1002/lno.10935,
589 2018.

590 Holm-Hansen, O., Lorenzen, C. J., and Holmes, J. D. H.: Fluorometric determination of
591 chlorophyll, ICES J. Mar. Sci., 30, 3-15, doi.org/10.1093/icesjms/30.1.3, 1965.

592 Ito, T., Parekh, P., Dutkiewicz, S., and Follows, M. J.: The Antarctic circumpolar productivity
593 belt, Geophys. Res. Lett., 32, L13604, doi:10.1029/2005gl023021, 2005.

594 Jakuba, R. W., Moffett, J. W., and Dyhrman, S. T.: Evidence for the linked biogeochemical
595 cycling of zinc, cobalt, and phosphorus in the western north Atlantic Ocean, Global
596 Biogeochem. Cy., 22, GB4012, doi:10.1029/2007GB003119, 2008.

597 Jakuba, R. W., Saito, M. A., Moffett, J. W., and Xu, Y.: Dissolved zinc in the subarctic North
598 Pacific and Bering Sea: Its distribution, speciation, and importance to primary producers,
599 Global Biogeochem. Cy., 26, GB2015, doi:10.1029/2010gb004004, 2012.

600 Lane, T. W., and Morel, F. M. M.: Regulation of carbonic anhydrase expression by zinc, cobalt,
601 and carbon dioxide in the marine diatom Thalassiosira weissflogii, Plant Physiol., 123, 345-
602 352, doi:10.1104/Pp.123.1.345, 2000.

603 Largier, J. L., Chapman, P., Peterson, W. T., and Swart, V. P.: The western Agulhas Bank:
604 circulation, stratification and ecology, S Afr J Marine Sci, 12, 319-339,
605 doi:10.2989/02577619209504709, 1992.

https://doi.org/10.5194/bg-2020-42
Preprint. Discussion started: 6 March 2020

606 Leblanc, K., Hare, C. E., Boyd, P. W., Bruland, K. W., Sohst, B., Pickmere, S., Lohan, M. C.,
607 Buck, K., Ellwood, M., and Hutchins, D. A.: Fe and Zn effects on the Si cycle and diatom
608 community structure in two contrasting high and low-silicate HNLC areas, Deep-Sea Res. Pt
609 I, 52, 1842-1864, doi:10.1016/j.dsr.2005.06.005, 2005.

610 Lee, J. G., and Morel, F. M. M.: Replacement of zinc by cadmium in marine phytoplankton,
611 Mar. Ecol. Prog. Ser., 127, 305-309, doi:10.3354/Meps127305, 1995.

612 Little, S. H., Vance, D., McManus, J., and Severmann, S.: Key role of continental margin
613 sediments in the oceanic mass balance of Zn and Zn isotopes, Geology, 44, 207-210,
614 doi:10.1130/G37493.1, 2016.

615 Lutjeharms, J. R. E.: Three decades of research on the greater Agulhas Current, Ocean Sci., 3,
616 129-147, doi:10.5194/os-3-129-2007, 2007.

617 Lutjeharms, J. R. E., and Cooper, J.: Interbasin leakage through Agulhas current filaments,
618 Deep-Sea Res. Pt I, 43, 213-238, doi:10.1016/0967-0637(96)00002-7, 1996.

619 Mackey, M. D., Mackey, D. J., Higgins, H. W., and Wright, S. W.: Chemtax - a program for
620 estimating class abundances from chemical markers: Application to HPLC measurements of
621 phytoplankton, Mar. Ecol. Prog. Ser., 144, 265-283, doi:10.3354/meps144265, 1996.

622 Mahaffey, C., Reynolds, S., Davis, C. E., and Lohan, M. C.: Alkaline phosphatase activity in
623 the subtropical ocean: Insights from nutrient, dust and trace metal addition experiments, Front.
624 Mar. Sci., 1, doi:10.3389/fmars.2014.00073, 2014.

625 Martiny, A. C., Lomas, M. W., Fu, W., Boyd, P. W., Chen, Y. L., Cutter, G. A., Ellwood, M.
626 J., Furuya, K., Hashihama, F., Kanda, J., Karl, D. M., Kodama, T., Li, Q. P., Ma, J., Moutin,
627 T., Woodward, E. M. S., and Moore, J. K.: Biogeochemical controls of surface ocean
628 phosphate, Sci. Adv., 5, eaax0341, doi:10.1126/sciadv.aax0341, 2019.

629 McLennan, S. M.: Relationships between the trace element composition of sedimentary rocks
630 and upper continental crust, Geochem. Geophy. Geosy., 2, doi:10.1029/2000gc000109, 2001.

631 Menzel Barraqueta, J. L., Klar, J. K., Gledhill, M., Schlosser, C., Shelley, R., Planquette, H.
632 F., Wenzel, B., Sarthou, G., and Achterberg, E. P.: Atmospheric deposition fluxes over the
633 Atlantic Ocean: A GEOTRACES case study, Biogeosciences, 16, 1525-1542, doi:10.5194/bg-
634 16-1525-2019, 2019.

635 Milne, A. C., Schlosser, C., Wake, B. D., Achterberg, E. P., Chance, R., Baker, A. R., Forryan,
636 A., and Lohan, M. C.: Particulate phases are key in controlling dissolved iron concentrations
637 in the (sub)tropical North Atlantic, Geophys. Res. Lett., 44, 2377-2387,
638 doi:10.1002/2016GL072314, 2017.

639 Moore, C. M.: Diagnosing oceanic nutrient deficiency., Philisophical Transactions of the Royal
640 Society A: Mathmatical, Physical and Engineering Sciences, 374, doi:10.1098/rsta.2015.0290,
641 2016.

642 Moore, C. M., Mills, M. M., Arrigo, K. R., Berman-Frank, I., Bopp, L., Boyd, P. W., Galbraith,
643 E. D., Geider, R. J., Guieu, C., Jaccard, S. L., Jickells, T. D., La Roche, J., Lenton, T. M.,
644 Mahowald, N. M., Marañón, E., Marinov, I., Moore, J. K., Nakatsuka, T., Oschlies, A., Saito,

https://doi.org/10.5194/bg-2020-42
Preprint. Discussion started: 6 March 2020

M. A., Thingstad, T. F., Tsuda, A., and Ulloa, O.: Processes and patterns of oceanic nutrient limitation, Nat. Geosci., 6, 701-710, doi:10.1038/ngeo1765, 2013.

Moore, J. K., and Abbott, M. R.: Phytoplankton chlorophyll distributions and primary production in the Southern Ocean, J. Geophys. Res-Oceans, 105, 28709-28722, doi:10.1029/1999jc000043, 2000.

Morel, F. M. M.: The co-evolution of phytoplankton and trace element cycles in the oceans, Geobiology, 6, 318-324, doi:10.1111/j.1472-4669.2008.00144.x, 2008.

Morel, F. M. M., Reinfelder, J. R., Roberts, S. B., Chamberlain, C. P., Lee, J. G., and Yee, D.: Zinc and carbon co-limitation of marine-phytoplankton, Nature, 369, 740-742, doi:10.1038/369740a0, 1994.

Noble, A. E., Ohnemus, D. C., Hawco, N. J., Lam, P. J., and Saito, M. A.: Coastal sources, sinks and strong organic complexation of dissolved cobalt within the US North Atlantic GEOTRACES transect GA03, Biogeosciences, 14, 2715–2739, doi:10.5194/bg-14-2715-2017, 2017.

Ohnemus, D. C., and Lam, P. J.: Cycling of lithogenic marine particles in the US GEOTRACES North Atlantic transect, Deep-Sea Res. Pt II, 116, 283-302, doi:10.1016/j.dsr2.2014.11.019, 2015.

Ohnemus, D. C., Auro, M. E., Sherrell, R. M., Lagerstrom, M., Morton, P. L., Twining, B. S., Rauschenberg, S., and Lam, P. J.: Laboratory intercomparison of marine particle digestions including Piranha: A novel chemical method for dissolution of polyethersulfone filters, Limnol. Oceanogr-Meth., 12, 530-547, doi:10.4319/lom.2014.12.530, 2014.

Palter, J. B., Sarmiento, J. L., Gnanadesikan, A., Simeon, J., and Slater, R. D.: Fueling export production: nutrient return pathways from the deep ocean and their dependence on the Meridional Overturning Circulation, Biogeosciences, 7, 3549-3568, doi:10.5194/bg-7-3549-2010, 2010.

Paul, M., van de Flierdt, T., Rehkämper, M., Khondoker, R., Weiss, D., Lohan, M. C., and Homoky, W. B.: Tracing the Agulhas leakage with lead isotopes, Geophys. Res. Lett., 42, 8515-8521, doi:10.1002/2015gl065625, 2015.

Price, N. M., and Morel, F. M. M.: Cadmium and cobalt substitution for zinc in a marine diatom, Nature, 344, 658-660, doi:10.1038/344658a0, 1990.

Raux, E., Schubert, H. L., and Warren*, M. J.: Biosynthesis of cobalamin (vitamin B12): A bacterial conundrum, Cell. Mol. Life Sci., 57, 1880-1893, doi:10.1007/PL00000670, 2000.

Rodionov, D. A., Vitreschak, A. G., Mironov, A. A., and Gelfand, M. S.: Comparative genomics of the vitamin B12 metabolism and regulation in prokaryotes, J. Biol. Chem., 278, 41148-41159, doi:10.1074/jbc.M305837200, 2003.

Saito, M. A., and Goepfert, T. J.: Zinc-cobalt colimitation of Phaeocystis antarctica, Limnol. Oceanogr., 53, 266-275, doi:10.4319/lo.2008.53.1.0266, 2008.

https://doi.org/10.5194/bg-2020-42
Preprint. Discussion started: 6 March 2020

682 Saito, M. A., and Moffett, J. W.: Temporal and spatial variability of cobalt in the Atlantic
683 Ocean, Geochim. Cosmochim. Ac., 66, 1943-1953, doi:10.1016/S0016-7037(02)00829-3,
684 2002.

685 Saito, M. A., Rocap, G., and Moffett, J. W.: Production of cobalt binding ligands in a
686 Synechococcus feature at the Costa Rica upwelling dome, Limnol. Oceanogr., 50, 279-290,
687 doi:10.4319/lo.2005.50.1.0279, 2005.

688 Saito, M. A., Moffett, J. W., Chisholm, S. W., and Waterbury, J. B.: Cobalt limitation and
689 uptake in Prochlorococcus, Limnol. Oceanogr., 47, 1629-1636,
690 doi:10.4319/lo.2002.47.6.1629, 2002.

691 Saito, M. A., Goepfert, T. J., Noble, A. E., Bertrand, E. M., Sedwick, P. N., and DiTullio, G.
692 R.: A seasonal study of dissolved cobalt in the Ross Sea, Antarctica: Micronutrient behavior,
693 absence of scavenging, and relationships with Zn, Cd, and P, Biogeosciences, 7, 4059-4082,
694 doi:10.5194/bg-7-4059-2010, 2010.

695 Saito, M. A., Noble, A. E., Hawco, N., Twining, B. S., Ohnemus, D. C., John, S. G., Lam, P.,
696 Conway, T. M., Johnson, R., Moran, D., and McIlvin, M.: The acceleration of dissolved
697 cobalt's ecological stoichiometry due to biological uptake, remineralization, and scavenging in
698 the Atlantic Ocean, Biogeosciences, 14, 4637-4662, doi:10.5194/bg-14-4637-2017, 2017.

699 Sarmiento, J. L., Gruber, N., Brzezinski, M. A., and Dunne, J. P.: High-latitude controls of
700 thermocline nutrients and low latitude biological productivity, Nature, 427, 56-60,
701 doi:10.1038/Nature02127, 2004.

702 Shaked, Y., Xu, Y., Leblanc, K., and Morel, F. M. M.: Zinc availability and alkaline
703 phosphatase activity in Emiliania huxleyi: Implications for Zn-P co-limitation in the ocean,
704 Limnol. Oceanogr., 51, 299-309, doi:10.4319/lo.2006.51.1.0299, 2006.

705 Sunda, W. G., and Huntsman, S. A.: Feedback interactions between zinc and phytoplankton in
706 seawater, Limnol. Oceanogr., 37, 25-40, doi:10.4319/lo.1992.37.1.0025 1992.

707 Sunda, W. G., and Huntsman, S. A.: Cobalt and zinc interreplacement in marine phytoplankton:
708 biological and geochemical implications, Limnol. Oceanogr., 40, 1404-1417,
709 doi:10.4319/lo.1995.40.8.1404, 1995.

710 Sunda, W. G., and Huntsman, S. A.: Control of Cd concentrations in a coastal diatom by
711 interactions among free ionic Cd, Zn, and Mn in seawater, Environ. Sci. Technol., 32, 2961-
712 2968, doi:10.1021/es980271y, 1998.

713 Sunda, W. G., and Huntsman, S. A.: Effect of Zn, Mn, and Fe on Cd accumulation in
714 phytoplankton: Implications for oceanic Cd cycling, Limnol. Oceanogr., 45, 1501-1516,
715 doi:10.4319/lo.2000.45.7.1501, 2000.

716 Tagliabue, A., Hawco, N. J., Bundy, R. M., Landing, W. M., Milne, A., Morton, P. L., and
717 Saito, M. A.: The role of external inputs and internal cycling in shaping the global ocean cobalt
718 distribution: insights from the first cobalt biogeochemical model, Global Biogeochem. Cy., 32,
719 594-616, doi:10.1002/2017gb005830, 2018.

720 Twining, B. S., and Baines, S. B.: The trace metal composition of marine phytoplankton, Annu.
721 Rev. Mar. Sci., 5, 191-215, doi:10.1146/annurev-marine-121211-172322, 2013.

https://doi.org/10.5194/bg-2020-42
Preprint. Discussion started: 6 March 2020

722 Vance, D., Little, S. H., de Souza, G. F., Khatiwala, S., Lohan, M. C., and Middag, R.: Silicon
723 and zinc biogeochemical cycles coupled through the Southern Ocean, Nat. Geosci., 10, 202-
724 206, doi:10.1038/ngeo2890, 2017.

725 Woodward, E. M. S., and Rees, A. P.: Nutrient distributions in an anticyclonic eddy in the
726 northeast Atlantic Ocean, with reference to nanomolar ammonium concentrations, Deep-Sea
727 Res. Pt II, 48, 775-793, doi:10.1016/S0967-0645(00)00097-7, 2001.

728 Wu, J. F., Sunda, W., Boyle, E. A., and Karl, D. M.: Phosphate depletion in the western North
729 Atlantic Ocean, Science, 289, 759-762, doi:10.1126/science.289.5480.759, 2000.

730 Wyatt, N. J., Milne, A., Woodward, E. M. S., Rees, A. P., Browning, T. J., Bouman, H. A.,
731 Worsfold, P. J., and Lohan, M. C.: Biogeochemical cycling of dissolved zinc along the
732 GEOTRACES South Atlantic transect GA10 at 40°S, Global Biogeochem. Cy., 28, 44-56,
733 doi:10.1002/2013gb004637, 2014.

734 Xu, Y., Tang, D., Shaked, Y., and Morel, F. M. M.: Zinc, cadmium, and cobalt
735 interreplacement and relative use efficiencies in the coccolithophore Emiliania huxleyi,
736 Limnol. Oceanogr., 52, 2294-2305, doi:10.4319/lo.2007.52.5.2294, 2007.

737 Zubkov, M. V., Fuchs, B. M., Tarran, G. A., Burkill, P. H., and Amann, R.: High rate of uptake
738 of organic nitrogen compounds by Prochlorococcus cyanobacteria as a key to their dominance
739 in oligotrophic oceanic waters, Appl. Environ. Microb., 69, 1299–1304,
740 doi:10.1128/aem.69.2.1299-1304.2003, 2003.

741

742

743 Table 1. Analytical validation results for open ocean surface seawater (SAFe S), 1000 m
744 seawater (SAFe D2) and 2000 m seawater (GEOTRACES GD). All concentrations are in nM
745 (± 1 std. dev.). ND indicates sample not determined.

746

	SAFe S	SAFe D2	GEOTRACES GD
Zn (FIA)	0.060 (0.020) *n* = 7	7.723 (0.091) *n* = 12	ND
Zn consensus value	0.071 (0.010)	7.634 (0.257)	1.757 (0.123)
Co (FIA)	0.004 (0.001) *n* = 3	0.049 (0.001) *n* = 2	0.073 (0.004) *n* = 5
Co consensus value	0.005 (0.001)	0.047 (0.003)	0.067 (0.001)

747

748

749 Table 2. Southeast Atlantic mixed-layer micro- and macronutrient mean concentrations during
750 early spring (D357-1), late spring (D357-2) and summer (JC068) transects alongside upper
751 water column ecological stoichiometries for Zn and Co calculated from linear regression with
752 PO_4^{3-} (see Sect. 3.4). Regression analysis was performed between the surface ocean and depth
753 that metal/PO_4^{3-} remained linear: 500 m for Zn/PO_4^{3-} and 360 m for Co/PO_4^{3-}. *r* indicates
754 Pearson's correlation coefficient.

https://doi.org/10.5194/bg-2020-42
Preprint. Discussion started: 6 March 2020

Oceanographic Regime	Transect	Zn (nmol m^{-3})	Co	NO^{3-} ($\mu mol\ m^{-3}$)	PO_4^{3-}	$Si(OH)_4$	Zn/PO_4^{3-} ($\mu M:M$)	*r*	Co/PO_4^{3-} ($\mu M:M$)	*r*	Zn:Co
STSW	Early spring	1597	30	870	203	2790	1150	0.69	39	0.83	29
	Late spring	625	18	658	191	2298	632	0.56	28	0.62	23
	Summer	184	26	22	117	1327	274	0.68	24	0.80	11
SASW	Early spring	123	15	4927	537	1865	276	0.59	31	0.62	9
	Summer	103	9	2786	417	786	302	0.76	34	0.81	9

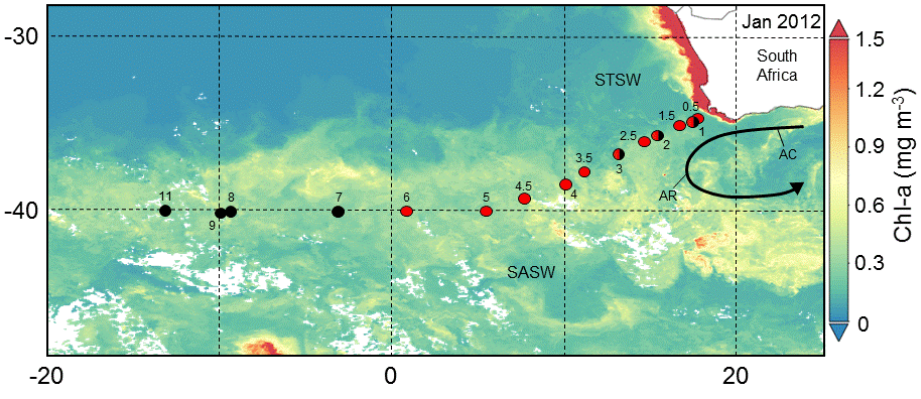

Figure 1. The Southeast Atlantic stations sampled for dissolved Zn and Co along the GA10 section during UK-GEOTRACES cruises D357 (red circles) and JC068 (black circles), overlain a VIIRS monthly composite image of chlorophyll-*a* concentrations for January 2012 (https://oceancolor.gsfc.nasa.gov/). Two transects were completed during D357 between Cape Town and the zero meridian that represent early austral spring 2010 (D357-1; Stns. 1, 2, 3, 4, 5 & 6) and late austral spring 2010 (D357-2; Stns. 0.5, 1, 1.5, 2.5, 3.5, 4.5), respectively. JC068 took place during austral summer 2011/12 and we present here only the repeat transect data between Cape Town and 13°W (Stns. 1, 2, 3, 7, 8, 9, 11). STSW = Sub-Tropical Surface Water, SASW = Sub-Antarctic Surface Water, AC = Agulhas Current, AR = Agulhas retroflection.

https://doi.org/10.5194/bg-2020-42
Preprint. Discussion started: 6 March 2020

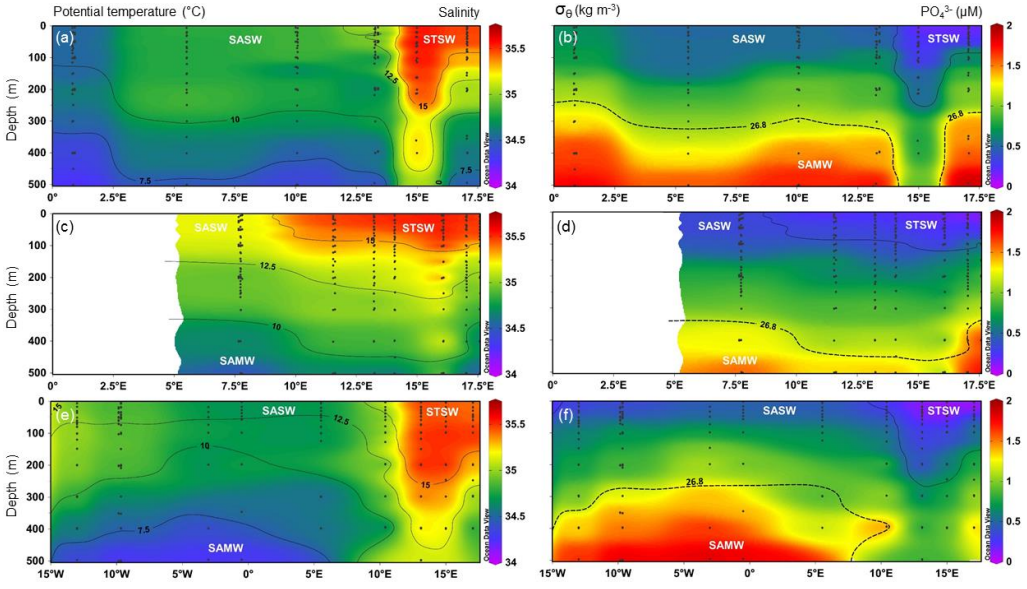

Figure 2. Upper 500 m thermohaline and dissolved PO_4^{3-} distributions for the Southeast Atlantic along the early spring (a,b; D357-1), late spring (c,d; D357-2) and summer (e,f; JC068) transects. The dominant Southern Ocean (SASW & SAMW) and South Atlantic (STSW) water masses that influence the distribution of nutrients are shown. The θ 15°C isotherm represents a practical definition of the STF location, whilst SAMW is identified by the median potential density isopycnal 26.8 kg m^{-3} (see Sect. 4.1.).

https://doi.org/10.5194/bg-2020-42
Preprint. Discussion started: 6 March 2020

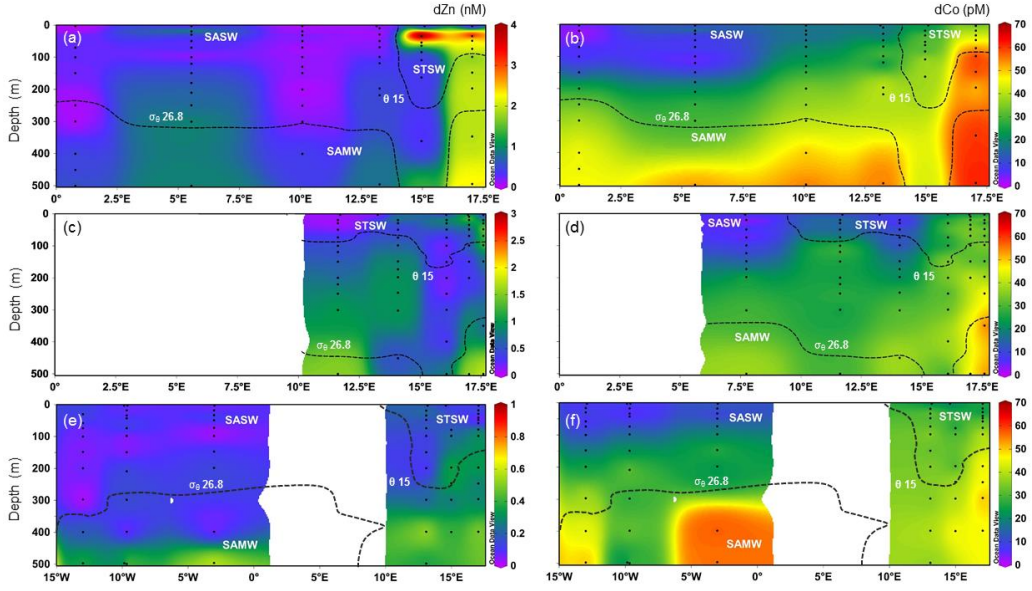

Figure 3. Upper 500 m dissolved Zn and Co distributions for the Southeast Atlantic along the early spring (a,b; D357-1), late spring (c,d; D357-2) and summer (e,f; JC068) transects. Note the change in dZn scale for E. The STF is delineated by θ 15°C, whilst the influence of SAMW is evident by the median potential density isopycnal 26.8 kg m^{-3} (see Section 4.1.).

https://doi.org/10.5194/bg-2020-42
Preprint. Discussion started: 6 March 2020

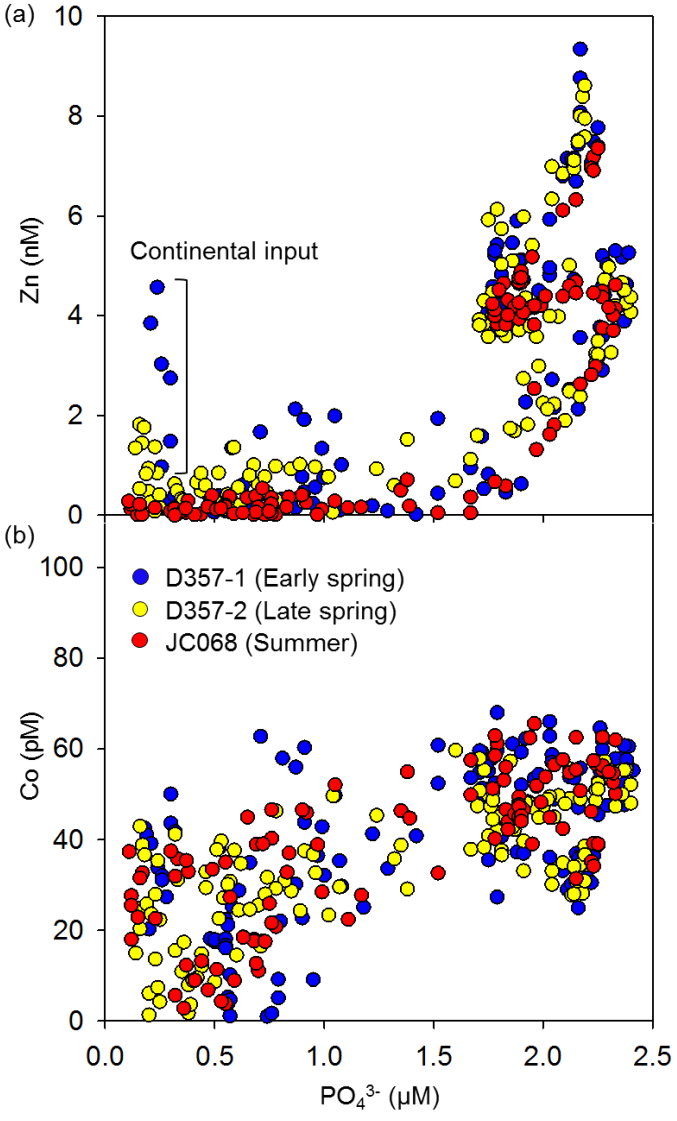

Figure 4. Full water column relationships between (a) dissolved Zn and PO_4^{3-} and (b) dissolved Co and PO_4^{3-} for the Southeast Atlantic during the early spring (blue circles; D357-1), late spring (yellow circles; D357-2) and summer (red circles; JCO68) transects.

https://doi.org/10.5194/bg-2020-42
Preprint. Discussion started: 6 March 2020

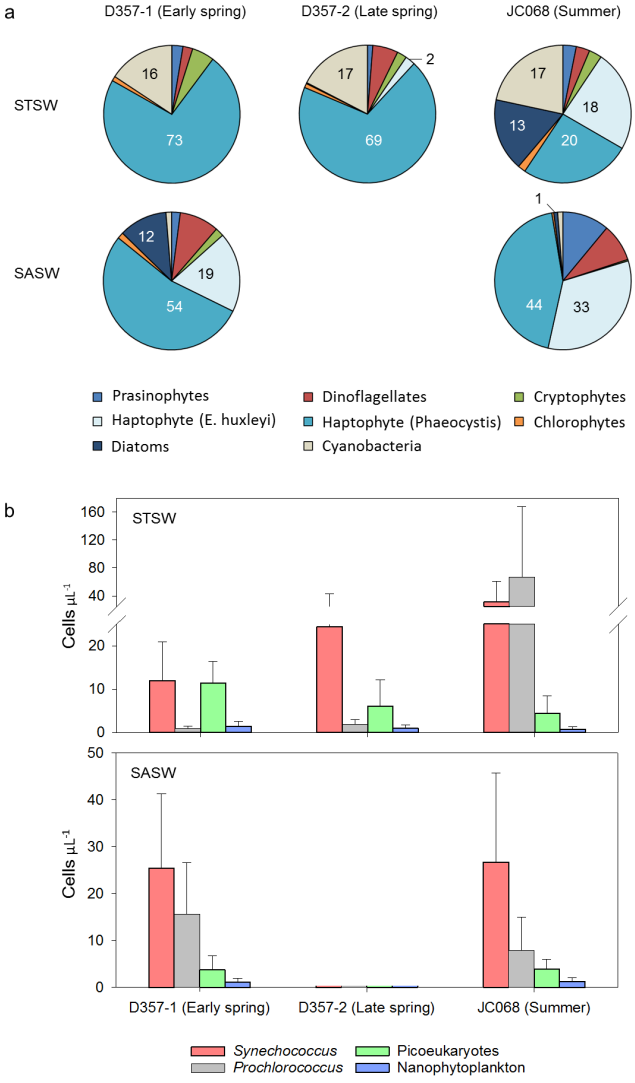

Figure 5. Seasonal differences in (a) pigment-derived taxonomic contributions to total chlorophyll-*a* (percentage), and (b) AFC counts of *Synechococcus*, *Prochlorococcus*, nanophytoplankton (approx. >2µm) and photosynthetic picoeukaryotes (approx. <2µm) in the Southeast Atlantic.

https://doi.org/10.5194/bg-2020-42
Preprint. Discussion started: 6 March 2020

Biogeosciences
Discussions
Open Access
EGU

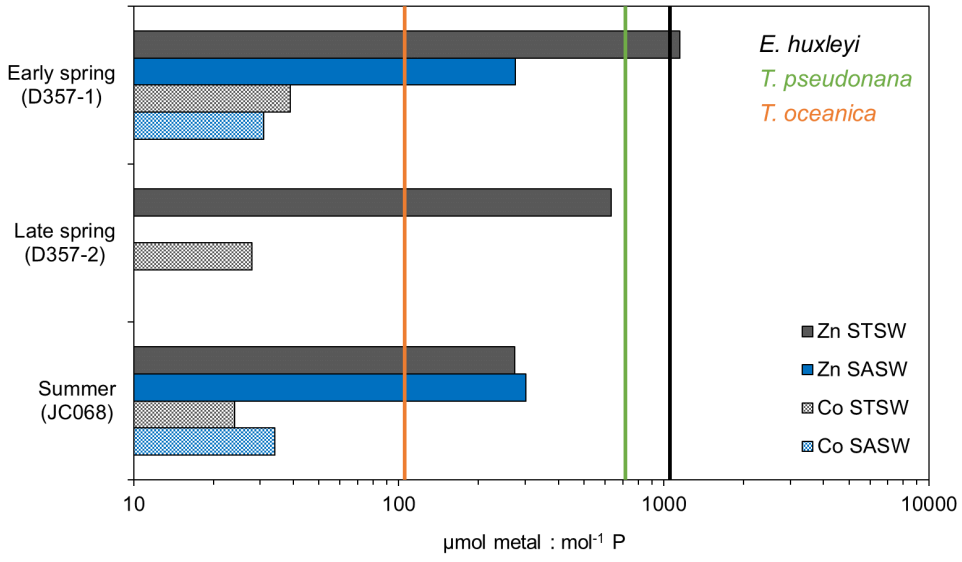

797

798 Figure 6. Ecological stoichiometries for dissolved Zn and Co in the upper water column of the
799 Southeast Atlantic (horizontal bars, Table 2) compared with laboratory estimates of cellular
800 Zn:P in eukaryotic phytoplankton below which growth limitation is observed (vertical lines,
801 no added Co to media; phytoplankton data from Sunda and Hunstman, 1995). This figure is
802 adapted from that in Saito et al. (2010) and implies that inter-seasonal differences in Zn:PO_4^{3-}
803 stoichiometries could impact phytoplankton community composition in STSW of the Southeast
804 Atlantic.